

Open Access Article. Published on 04/20/2023. Downloaded on 04/27/2023 10:06:31.
This article is licensed under a Creative Commons Attribution 3.0 Unported Licence.



[View Article Online](#)
[View Journal](#) | [View Issue](#)

Faraday Discussions

Volume: 245

Astrochemistry at high resolution



deuterated versions of $c\text{-C}_3\text{H}_3^+$, followed again by dissociative recombination. Observational proof of these hypotheses could not be obtained to date, as $c\text{-C}_3\text{H}_3^+$ has no permanent electric dipole moment and can thus only be detected in the infrared region.⁷ Its isotopically substituted versions, in particular $c\text{-C}_3\text{H}_2\text{D}^+$, have a small dipole moment, but high-resolution microwave laboratory data for these are still missing.

In this work, we provide the first rovibrational and pure rotational data for $c\text{-C}_3\text{H}_2\text{D}^+$, detected by a novel action spectroscopic method. The search for the spectral fingerprints was facilitated by the accurate *ab initio* predictions by Huang and Lee⁸ reported previously.

2 Experimental methods

The rovibrational and rotational transitions of $c\text{-C}_3\text{H}_2\text{D}^+$ were measured in the 4 K 22-pole trap instrument COLTRAP, which has been previously described in detail by Asvany *et al.*^{9,10} and will only be briefly explained here. Ions were generated in a storage ion source by electron impact ionization ($E_e \approx 30$ eV) of a precursor 1 : 1 mixture of singly deuterated acetylene, HCCD (CDN isotopes Inc.; which over time had become a mixture of HCCH, HCCD and DCCD), and methane, CH_4 . This mixture yielded excellent ion production conditions, possibly due to efficient reactions of the form $\text{CH}_3^+ + \text{HCCD} \rightarrow c\text{-C}_3\text{H}_2\text{D}^+ + \text{H}_2$ (Ali *et al.*¹¹). Every second, a pulse of up to a hundred thousand mass-selected $c\text{-C}_3\text{H}_2\text{D}^+$ ions ($m = 40$ u) was injected into the 4 K cold 22-pole ion trap. The trap was filled constantly with He ($n \approx 10^{13} \text{ cm}^{-3}$), and additionally a 1 : 3 Ne : He gas mixture was pulsed into the trap through a piezoelectrically actuated valve at the beginning of each trapping cycle.

Once trapped, the rovibrational transitions of $c\text{-C}_3\text{H}_2\text{D}^+$ were detected using a novel and very sensitive action spectroscopic method, called leak-out spectroscopy (LOS¹²). This method is based on the escape of a trapped ion after collision-induced transfer of vibrational into kinetic energy. After a cooling period of about 40 ms, the ions were irradiated for 500 ms by an IR beam traversing the trap. During this irradiation time, vibrationally excited $c\text{-C}_3\text{H}_2\text{D}^+$ ions will eventually be quenched by collisions with the Ne atoms present in the trap. Due to the neutral-to-ion mass ratio of 20 : 40, a substantial part of the vibrational energy is transferred into kinetic energy of the ion, namely a maximum of $20/(20 + 40) \times 3170 \text{ cm}^{-1} = 1057 \text{ cm}^{-1} \approx 0.131$ eV. By keeping the potential difference between the exit electrode and the floating potential of the trap well below 131 mV, the ions may escape in that direction so that they fly towards the ion detector where they are counted. By repeating these trapping cycles at 1 Hz and counting the escaping $c\text{-C}_3\text{H}_2\text{D}^+$ ions as a function of the laser wavenumber, a rovibrational spectrum was recorded.

The narrow-band IR radiation was generated by a continuous-wave optical parametric oscillator (cw-OPO, Aculight Argos Model 2400, module C). The IR beam entered the vacuum environment of the ion-trap machine *via* a 0.6 mm thick diamond window (Diamond Materials GmbH), irradiated the trapped ions by crossing the 22-pole trap, and exited the trap instrument *via* a CaF_2 window, after which it was absorbed by a power meter. The detected power was on the order of 200 mW. The frequency of the IR radiation was measured by a Bristol model 621A wavemeter with an accuracy of about 0.001 cm^{-1} (in well-adjusted



settings). We did additional calibration measurements with neutral C_2H_2 contained in a gas cell after the IR data reported here was measured. The exact frequencies for C_2H_2 are given in the HITRAN database¹³ and, following this calibration, we shifted our data up by 0.007 cm^{-1} . With this, the accuracy of the given IR data should be on the order of 0.001 cm^{-1} .

For detecting pure rotational transitions, we used a novel double-resonance scheme¹⁴ based on LOS, as recently described in Asvany *et al.*¹⁵. A rubidium-clock-referenced microwave synthesizer (Rohde & Schwarz SMF100A) driving an amplifier-multiplier chain (Virginia Diodes Inc. WR9.0M-AMC, WR4.3x2) was used to generate the mm-wave radiation. The radiation was focused by an ellipsoidal mirror ($f = 43.7\text{ mm}$ (ref. 16)) before entering the vacuum environment through the diamond window. Both the IR and mm-wave radiation sources were used simultaneously, and their beams combined by a small hole in the ellipsoidal mirror through which the narrow IR beam could pass. The frequency of the IR photons is kept fixed on a rovibrational transition starting from a rotational level of the vibrational ground state, resulting in a detectable and constant LOS signal. The mm-wave photon then excites a rotational transition starting or ending on the rotational quantum state probed by the IR laser, thus decreasing or increasing the LOS signal, respectively. A rotational line can therefore be recorded by modulating this LOS signal, *i.e.*, by scanning the frequency of the mm-wave source, as will be shown in section 3.2.

3 Experimental measurements

3.1 Rovibrational measurements

$c\text{-}C_3H_2D^+$ is a near-oblate asymmetric top (C_{2v} symmetry) with 12 fundamental vibrational modes, none of which have been measured previously in the gas phase, to the best of our knowledge. A previous infrared experimental study for $C_3H_2D^+$ was done in 1986 by Craig *et al.*¹⁷ in the solution phase, but its vibrational band centres are subject to shifts. Based on the spectroscopic predictions of Huang and Lee,⁸ we detect the symmetric C–H stretch ν_1 (vibrational symmetry a_1 , a-type transition) at high spectral resolution. The spectrum was measured in the range of our $3\text{ }\mu\text{m}$ OPO over multiple scans ranging over $1.5\text{--}2\text{ cm}^{-1}$ and is depicted in Fig. 1. In total, 126 lines were assigned in the ν_1 fundamental band of $c\text{-}C_3H_2D^+$, covering a range of 20 cm^{-1} . The observed and assigned line positions are given in the ESI† together with the fit residuals (see section 4 for the final fit).

Apart from the ν_1 lines of $c\text{-}C_3H_2D^+$, additional lines with seemingly characteristic patterns were observed in the spectrum. Based on our mass selectivity ($m = 40\text{ u}$) and by considering the possible isomers that could be formed in the source during the ionization of the precursor mixture, we believe that the remaining lines are presumably from singly deuterated $l\text{-}C_3H_3^+$, $l\text{-}HDC_3H^+$ or $l\text{-}H_2C_3D^+$. We tentatively assign the additional features to the $l\text{-}HDC_3H^+$ form (simulated as blue sticks in Fig. 1), based on theoretical predictions for both isomers of $l\text{-}C_3H_2D^+$ reported by Huang and Lee.⁸ But due to perturbations in the measured spectrum, a definitive assignment needs further investigation, and we postpone the discussion of the $l\text{-}C_3H_2D^+$ species to a forthcoming publication. Additionally, due to the high sensitivity of LOS, some weak lines were seen that could not be assigned to either $c\text{-}C_3H_2D^+$ or $l\text{-}HDC_3H^+$. These might be perturbed



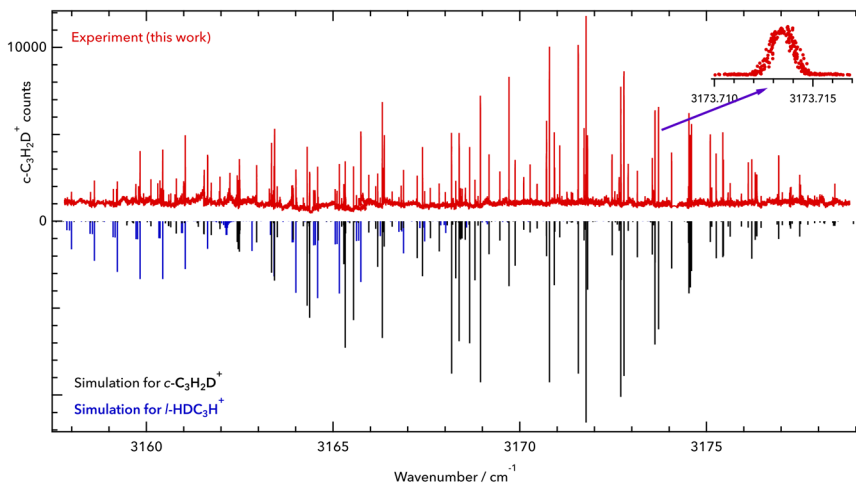


Fig. 1 Rovibrational spectrum of the symmetric C–H stretching vibration of $c\text{-C}_3\text{H}_2\text{D}^+$. Upper part: experimental data of this work (red). Lower part: PGOPHER simulation at a rotational temperature of $T = 10$ K (black sticks). The band origin was found to be at 3168.565 cm^{-1} . The zoomed-in inset shows the line $4_{13} \leftarrow 3_{12}$ of the $\nu_1 = 1 \leftarrow 0$ band at 3173.714 cm^{-1} . Some additional lines have been detected, which are tentatively assigned here to $l\text{-HDC}_3\text{H}^+$ (blue sticks). The red trace is provided as a separate data file in the ESI.†

lines of the $l\text{-HDC}_3\text{H}^+$ band, or some combination or overtone bands of lower vibrational states of $c\text{-C}_3\text{H}_2\text{D}^+$.

Because of the low temperature of the ion trap, the transitions exhibit narrow Doppler widths. One example is the line $4_{13} \leftarrow 3_{12}$ of the $\nu_1 = 1 \leftarrow 0$ band at 3173.714 cm^{-1} , which is depicted in the inset of Fig. 1. This line has a full width at half maximum (FWHM) of about 40 MHz, corresponding to a kinetic temperature of 12 K. This temperature is slightly higher than the nominal trap temperature due to known heating effects.¹⁸

3.2 Rotational measurements

$c\text{-C}_3\text{H}_2\text{D}^+$ is predicted to have a dipole moment component of 0.225 Debye along its a -axis⁸ and should therefore feature weak a -type rotational transitions. Such rotational transitions can be measured in ion traps using double-resonance schemes,¹⁴ as demonstrated in our group by several examples.^{19,20} The double-resonance scheme using LOS, as applied in this work, has been demonstrated only recently.¹⁵ Example transitions recorded by applying this double-resonance scheme are shown in Fig. 2.

Such spectra were recorded in multiple individual measurements in which the mm-wave frequency (blue arrows in Fig. 2) was stepped in an up-and-down manner several times in a given frequency window; the frequency steps were kept constant in individual experiments, and varied between 2 and 10 kHz. Selected rovibrational lines from the ν_1 band were used for the IR excitation (red arrows in Fig. 2). The spectroscopic data were normalized employing a frequency-switching procedure, *i.e.*, by dividing the $c\text{-C}_3\text{H}_2\text{D}^+$ counts monitored while scanning the spectral window of interest by the counts at an off-resonant mm-wave reference frequency. Therefore, the baselines in Fig. 2 are close to unity.



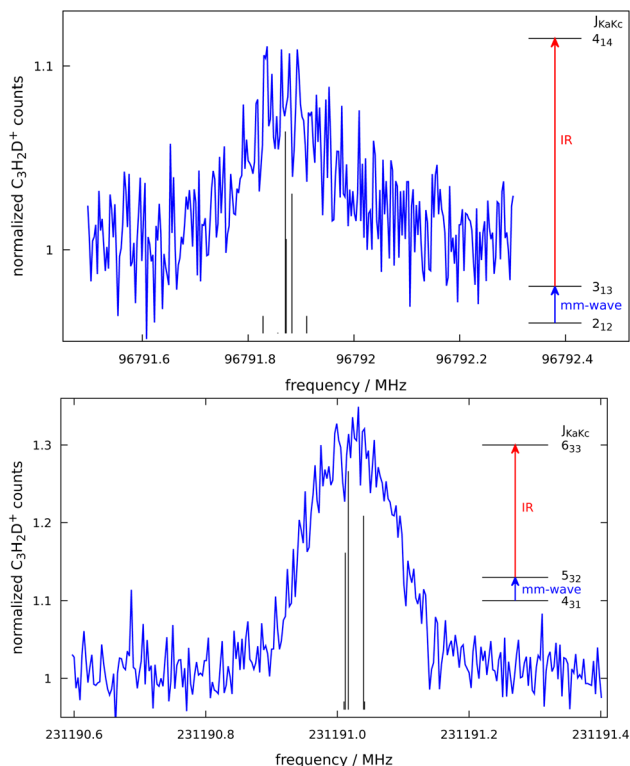


Fig. 2 Pure rotational transitions $J_{K_a K_c} = 3_{13} \leftarrow 2_{12}$ and $J_{K_a K_c} = 5_{32} \leftarrow 4_{31}$ of $c\text{-C}_3\text{H}_2\text{D}^+$ measured by a double-resonance scheme, in which the mm-wave excitation (blue arrows in insets) is followed by IR excitation (red arrows in insets) into the ν_1 vibrational band and subsequent leak-out from the trap. The step sizes are 3 kHz in both cases. The signal counts are normalized and therefore the baseline is unity. The calculated hyperfine structure of the lines are indicated by black sticks. The $J_{K_a K_c} = 3_{13} \leftarrow 2_{12}$ line is power-broadened.

Subsequently, the normalized counts of one measurement were averaged for each given frequency position. The obtained on-resonance signal enhancement is on the order of 8% to 30%, as seen in Fig. 2. Transition frequencies were determined by adjusting the parameters of an appropriate line-shape function (a Gaussian) to the experimental spectrum in a least-squares procedure. In total, 16 rotational lines have been detected, which are summarised in Table 1 and depicted in Fig. 3. The frequencies and their uncertainties in Table 1 result from several (about 3 to 10) independent measurements for each line.

4 Spectroscopic parameters

To obtain accurate spectroscopic parameters for the ground and first excited vibrational states of $c\text{-C}_3\text{H}_2\text{D}^+$, we carried out fits of the experimental transition frequencies using a Watson's S-reduced Hamiltonian in the I' representation as implemented in the PGOPHER program.²¹ Initially, the rovibrational lines were assigned using the assistance of *ab initio* calculations from Huang and Lee.⁸ A first



Table 1 Measured low-lying rotational transitions of $c\text{-C}_3\text{H}_2\text{D}^+$ (in MHz). In total, 16 rotational lines have been measured directly by the double resonance technique. Uncertainties are given in parentheses. The obs-calc values are the difference between the observed transition frequency and the calculated frequency using the fitted rotational constants

$J_{K_a K_c} \leftarrow J_{K_a K_c}$	This work	obs-calc
$2_{11} \leftarrow 1_{10}$	90 293.296(15)	0.0283
$3_{13} \leftarrow 2_{12}$	96 791.884(15)	0.0235
$3_{03} \leftarrow 2_{02}$	97 972.838(15)	0.0190
$3_{22} \leftarrow 2_{21}$	118 087.007(10)	0.0090
$4_{14} \leftarrow 3_{13}$	125 054.348(10)	0.0071
$5_{24} \leftarrow 4_{23}$	180 356.9896(34)	-0.0024
$6_{16} \leftarrow 5_{15}$	180 733.6130(07)	-0.0005
$6_{06} \leftarrow 5_{05}$	180 737.9305(16)	0.0021
$4_{22} \leftarrow 3_{21}$	181 026.5963(24)	-0.0007
$5_{14} \leftarrow 4_{13}$	181 735.1075(07)	-0.0001
$4_{31} \leftarrow 3_{30}$	182 399.3395(19)	-0.0002
$3_{30} \leftarrow 2_{11}$	197 358.1392(25)	0.0001
$5_{33} \leftarrow 4_{32}$	202 928.5429(21)	0.0001
$7_{17} \leftarrow 6_{16}$	208 526.1574(26)	0.0003
$6_{15} \leftarrow 5_{14}$	208 882.1638(36)	0.0033
$5_{32} \leftarrow 4_{31}$	231 191.0231(09)	0.0001

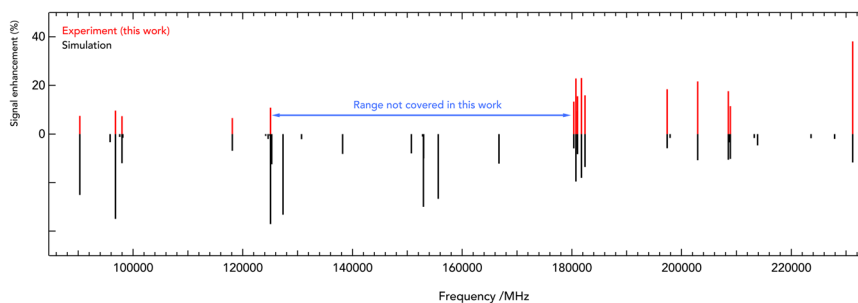


Fig. 3 Stick spectra of the pure rotational transitions of $c\text{-C}_3\text{H}_2\text{D}^+$ measured between 90 and 230 GHz. The experimental frequencies (in red, top) are compared to a PGOPHER simulation at 10 K (black, bottom). The experimental intensities are given as signal enhancement of the normalized ion counts (as in Fig. 2). The regions 90–125 GHz and 175–230 GHz were collected using two different multiplier chain settings and no experimental measurement was done for 125–170 GHz.

fit of these data was then used to predict the pure rotational transition frequencies of $c\text{-C}_3\text{H}_2\text{D}^+$ in the ground vibrational state. The best-fit ground-state molecular parameters were determined using the pure rotational transition frequencies given in Table 1 together with ground-state combination differences from the IR measurements. As the low-frequency measurements (up to 125 GHz) are affected by power broadening, transition frequencies are thought to be accurate only within 10–15 kHz, while the uncertainties for the measurements at higher frequencies are smaller. The overall rms of the fit is 0.0008 cm^{-1} for the IR combination differences and 11 kHz for the pure rotational data. The complete



Table 2 The best-fit spectroscopic parameters (in Watson's *S*-reduction) for the ground and first vibrationally excited state (C–H symmetric stretch) of $c\text{-C}_3\text{H}_2\text{D}^+$ obtained by fitting our data with the program PGOPHER.²¹ All values are in MHz, except for the band origin of ν_1 , which is given in cm^{-1} . The numbers in parentheses give the uncertainty of the last digits. Our values are compared to the accurate *ab initio* predictions of Huang and Lee⁸

Parameter	Experimental		Calculated ⁸	
	Ground state	ν_1	Ground state	ν_1
ν_0	0	3168.56489(19)	0	3164.8/3173.1
A	30 747.25030(85)	30 586.58(69)	30 757	30 625
B	25 465.51589(40)	25 421.40(56)	25 478	25 442
C	13 897.86084(23)	13 859.82(24)	13 901	13 864
α^A		160.67(69)		131.92
α^B		44.12(56)		36.02
α^C		38.04(24)		37.57
D_J	0.014734(6)	^a	0.0145	
D_{JK}	0.08525(5)	^a	0.084	
D_K	−0.02599(7)	^a	−0.026	
d_1	−0.010248(3)	^a	−0.010018	
d_2	−0.005259(3)	^a	−0.005106	
χ_{aa} (D)	0.187 ^b			
χ_{bb} (D)	−0.100 ^b			
χ_{cc} (D)	−0.087 ^b			

^a The distortion constants of the ν_1 state have been fixed to those determined for the ground state. ^b Nuclear quadrupole coupling constants of the deuterium nucleus calculated at the ae-CCSD(T)/cc-pwCVQZ level.

parameter set is given in Table 2. Hyperfine structure from the presence of the deuterium nucleus ($I_{\text{D}} = 1$) was not resolved in our measurements (*cf.* Fig. 2). For the sake of completeness, deuterium ($I_{\text{D}} = 1$) quadrupole coupling constants that were estimated at the CCSD(T)/cc-pwCVQZ level of theory (considering all electrons in the correlation treatment) using the CFOUR program²² are also given in Table 2. The corresponding structural parameters at this level are $r_{\text{C-C}} = 1.36024 \text{ \AA}$ and $r_{\text{C-H}} = 1.07828 \text{ \AA}$.

After obtaining the ground-state spectroscopic parameters, the band origin and rotational constants for the ν_1 vibrationally excited state were determined in a second fitting procedure. In this fit, the distortion constants in ν_1 have simply been fixed to those determined for the ground state. The derived spectroscopic parameters for the ground and ν_1 states are summarized in Table 2 along with the theoretical predictions from Huang and Lee.⁸ The line lists of transition frequencies and residuals for both fits are provided in the ESI file.† Overall, the experimentally derived constants show excellent agreement with the calculated values, providing extra confirmation for the unequivocal detection of $c\text{-C}_3\text{H}_2\text{D}^+$ here.

5 Discussion and outlook

Leak-out spectroscopy (LOS) is a novel method for spectroscopy in ion traps, which features general applicability and high sensitivity. This is demonstrated here for the astronomically important $c\text{-C}_3\text{H}_2\text{D}^+$ molecule, which has evaded



spectroscopic detection by other methods so far. The excellent signal quality (the background in Fig. 1 is on the order of 1000 $c\text{-C}_3\text{H}_2\text{D}^+$ counts per trapping cycle, while the signal is on the order of 11 000 counts for the strongest rovibrational lines) allowed the complete IR spectrum, shown in Fig. 1, to be recorded within a few days. Also, subsequent measurements of its 16 rotational lines in the ground state provide the first experimental rotational spectrum, which will be useful for the astronomical community.

As mentioned in the introduction, $c\text{-C}_3\text{H}_2$ is a molecule relevant for the chemistry of cold interstellar environments,^{23,24} which is thought to be formed from $c\text{-C}_3\text{H}_3^+$ by dissociative recombination with an electron. But while the abundant $c\text{-C}_3\text{H}_2$ has a very large permanent dipole moment of 3.43 D (ref. 25) and was thus detected in the early days of radio astronomy, $c\text{-C}_3\text{H}_3^+$ (D_{3h} point-group symmetry) has no permanent dipole moment making its identification through rotational spectroscopy or radio astronomy impossible. The recently launched James Webb Space Telescope (JWST) offers higher sensitivity for the infrared region, which might aid the detection of $c\text{-C}_3\text{H}_3^+$ using its high-resolution rovibrational spectrum.⁷

Inclusion of one ^{13}C or one D atom in the structure of $c\text{-C}_3\text{H}_3^+$ imparts a non-zero dipole moment component in the isotopologues. In the case of $c\text{-C}_3\text{H}_2\text{D}^+$, this dipole moment is calculated to be 0.225 D,⁸ which opens up the possibility for its search in various interstellar environments by its rotational fingerprints. This may be especially relevant for regions where other carbocations, such as $l\text{-C}_3\text{H}^+$ and the neutral $c\text{-C}_3\text{H}_2$ (and its isotopologues), have been detected.^{6,26,27} These future detections could provide crucial inputs to improve low-temperature chemical models, and potentially highlight which reactions and their deuterated versions play a significant role in the hydrocarbon chemistry in these environments.

Among the different $c\text{-C}_3\text{H}_3^+$ isotopologues, given the dipole moment and elemental isotope abundances, it would seem that $c\text{-C}_3\text{H}_2\text{D}^+$ should be the easiest species to be identified in an astronomical spectrum. It is worth noting that its dipole moment is essentially twice that of carbon monoxide, which has a dipole moment of only 0.122 D.²⁴ For the warm carbon chain chemistry in the protostar L1527, a column density of $\sim 10^{12} \text{ cm}^{-2}$ is determined for $c\text{-C}_3\text{HD}$ by Sakai *et al.*,²⁶ implying a column density of $\sim 10^{10} \text{ cm}^{-2}$ for $c\text{-C}_3\text{H}_2\text{D}^+$ (Aikawa, private communication, based on her model²⁸). Similarly, for the colder pre-stellar core L1544, based on the abundance of $c\text{-C}_3\text{HD}$ ($\sim 4\text{--}6 \times 10^{12} \text{ cm}^{-2}$; Spezzano *et al.*,⁶ and Giers *et al.*²⁹), and available astrochemical models,^{3,28} a column density in the order of $3 \times 10^{10} \text{ cm}^{-2}$ is estimated for $c\text{-C}_3\text{H}_2\text{D}^+$. This low column density in combination with the small dipole moment and the diluted spectral signature of this asymmetric top molecule results in integration times for strong selected lines in excess of several hundred hours for a single-dish telescope such as the IRAM 30 m facility (Schilke, Kim; private communication), rendering its current radio-astronomical detection very challenging. Indeed, this molecule has not been found in the deep surveys QUIJOTE³¹ and GOTHAM³² of TMC-1 (Cernicharo and McGuire, respectively, private communication).

Nevertheless, the first rotational spectra for this molecule obtained here lays the groundwork for future astronomical searches. The high sensitivity of the novel LOS method, with the possibility to be used also in an infrared-millimetre-wave double-resonance fashion, will also enable new investigations of challenging molecular ions relevant to astrochemistry. A recent example from our



laboratory concerns another member of the $C_3H_3^+$ family, namely open-chain $H_2C_3H^+$, which is thought to be the precursor for $I-C_3H_2$ in space.³⁰ A publication about its rovibrational and rotational signatures is in preparation.

Author contributions

Divita Gupta: writing – original draft, methodology, investigation, formal analysis, visualization, validation, writing – review & editing. Wesley G. D. P. Silva: writing – original draft, formal analysis, investigation, visualization, validation, writing – review & editing. José L. Doménech: investigation, validation, writing – review & editing. Eline Plaar: investigation, writing – review & editing. Sven Thorwirth: validation, writing – review & editing. Stephan Schlemmer: conceptualization, funding acquisition, project administration, supervision, writing – review & editing. Oskar Asvany: conceptualization, funding acquisition, validation, methodology, supervision, writing – original draft, writing – review & editing.

Conflicts of interest

There are no conflicts to declare.

Acknowledgements

This work has been supported *via* Collaborative Research Centre 956, sub-project B2, funded by the Deutsche Forschungsgemeinschaft (DFG, project ID 184018867) and DFG SCHL 341/15-1 (“Cologne Center for Terahertz Spectroscopy”). The Cologne group acknowledges the ERC advanced grant (MissIons: 101020583) for funding. W. G. D. P. S. thanks the Alexander von Humboldt Foundation for support through a postdoctoral fellowship. J. L. D. acknowledges the support from the MCINN project PID2020-113084GB-I00 and the CSIC project I LINK+ LINKA20353. We thank Peter Schilke, Wonju Kim, Yuri Aikawa, José Cernicharo, Brett McGuire and Silvia Spezzano for discussions about the feasibility of detecting $c-C_3H_2D^+$ in space.

Notes and references

- 1 P. Thaddeus, M. Guelin and R. A. Linke, *Astrophys. J.*, 1981, **246**, L41–L45.
- 2 P. Thaddeus, J. M. Vrtilek and C. A. Gottlieb, *Astrophys. J.*, 1985, **299**, L63–L66.
- 3 O. Sipilä, S. Spezzano and P. Caselli, *Astron. Astrophys.*, 2016, **591**, L1.
- 4 J. Gómez-González, M. Guélin, J. Cernicharo, C. Kahane and M. Bogey, *Astron. Astrophys.*, 1986, **168**, L11.
- 5 M. B. Bell, P. A. Feldman, H. E. Matthews and L. W. Avery, *Astrophys. J.*, 1986, **311**, L89.
- 6 S. Spezzano, S. Brünken, P. Schilke, P. Caselli, K. M. Menten, M. C. McCarthy, L. Bizzocchi, S. P. Treviño-Morales, Y. Aikawa and S. Schlemmer, *Astrophys. J., Lett.*, 2013, **769**, L19.
- 7 D. Zhao, K. D. Doney and H. Linnartz, *Astrophys. J., Lett.*, 2014, **791**, L28.
- 8 X. Huang and T. J. Lee, *Astrophys. J.*, 2011, **736**, 33.
- 9 O. Asvany, F. Bielau, D. Moratschke, J. Krause and S. Schlemmer, *Rev. Sci. Instrum.*, 2010, **81**, 076102.



- 10 O. Asvany, S. Brünken, L. Kluge and S. Schlemmer, *Appl. Phys. B*, 2014, **114**, 203–211.
- 11 A. Ali, E. C. Sittler, D. Chornay, B. R. Rowe and C. Puzzarini, *Planet. Space Sci.*, 2013, **87**, 96–105.
- 12 P. C. Schmid, O. Asvany, T. Salomon, S. Thorwirth and S. Schlemmer, *J. Phys. Chem. A*, 2022, **126**, 8111–8117.
- 13 I. Gordon, L. Rothman, R. Hargreaves, R. Hashemi, E. Karlovets, F. Skinner, E. Conway, C. Hill, R. Kochanov, Y. Tan, P. Wcisło, A. Finenko, K. Nelson, P. Bernath, M. Birk, V. Boudon, A. Campargue, K. Chance, A. Coustenis, B. Drouin, J. Flaud, R. Gamache, J. Hodges, D. Jacquemart, E. Mlawer, A. Nikitin, V. Perevalov, M. Rotger, J. Tennyson, G. Toon, H. Tran, V. Tyuterev, E. Adkins, A. Baker, A. Barbe, E. Canè, A. Császár, A. Dudaryonok, O. Egorov, A. Fleisher, H. Fleurbaey, A. Foltynowicz, T. Furtenbacher, J. Harrison, J. Hartmann, V. Horneman, X. Huang, T. Karman, J. Karns, S. Kassi, I. Kleiner, V. Kofman, F. Kwabia-Tchana, N. Lavrentieva, T. Lee, D. Long, A. Lukashetskaya, O. Lyulin, V. Makhnev, W. Matt, S. Massie, M. Melosso, S. Mikhailenko, D. Mondelain, H. Müller, O. Naumenko, A. Perrin, O. Polyansky, E. Raddaoui, P. Raston, Z. Reed, M. Rey, C. Richard, R. Tóbiás, I. Sadiek, D. Schwenke, E. Starikova, K. Sung, F. Tamassia, S. Tashkun, J. Vander Auwera, I. Vasilenko, A. Viganin, G. Villanueva, B. Vispoel, G. Wagner, A. Yachmenev and S. Yurchenko, *J. Quant. Spectrosc. Radiat. Transfer*, 2022, **277**, 107949.
- 14 O. Asvany and S. Schlemmer, *Phys. Chem. Chem. Phys.*, 2021, **23**, 26602–26622.
- 15 O. Asvany, S. Thorwirth, P. C. Schmid, T. Salomon and S. Schlemmer, 2023, submitted to PCCP.
- 16 P. Jusko, O. Asvany, A.-C. Wallerstein, S. Brünken and S. Schlemmer, *Phys. Rev. Lett.*, 2014, **112**, 253005.
- 17 N. C. Craig, J. Pranata, S. J. Reinganum, J. R. Sprague and P. S. Stevens, *J. Am. Chem. Soc.*, 1986, **108**, 4378–4386.
- 18 O. Asvany and S. Schlemmer, *Int. J. Mass Spectrom.*, 2009, **279**, 147–155.
- 19 C. Markus, S. Thorwirth, O. Asvany and S. Schlemmer, *Phys. Chem. Chem. Phys.*, 2019, **21**, 26406–26412.
- 20 P. Jusko, A. Stoffels, S. Thorwirth, S. Brünken, S. Schlemmer and O. Asvany, *J. Mol. Spectrosc.*, 2017, **332**, 59–66.
- 21 C. M. Western, *J. Quant. Spectrosc. Radiat. Transfer*, 2017, **186**, 221–242.
- 22 D. A. Matthews, L. Cheng, M. E. Harding, F. Lipparini, S. Stopkowicz, T.-C. Jagau, P. G. Szalay, J. Gauss and J. F. Stanton, *J. Chem. Phys.*, 2020, **152**, 214108.
- 23 J. Pety, P. Gratier, V. Guzmán, E. Roueff, M. Gerin, J. R. Goicoechea, S. Bardeau, A. Sievers, F. Le Petit, J. Le Bourlot, A. Belloche and D. Talbi, *Astron. Astrophys.*, 2012, **548**, A68.
- 24 J. Muentzer, *J. Mol. Spectrosc.*, 1975, **55**, 490–491.
- 25 H. Kanata, S. Yamamoto and S. Saito, *Chem. Phys. Lett.*, 1987, **140**, 221–224.
- 26 N. Sakai, T. Sakai, T. Hirota and S. Yamamoto, *Astrophys. J.*, 2009, **702**, 1025.
- 27 S. Brünken, L. Kluge, A. Stoffels, O. Asvany and S. Schlemmer, *Astrophys. J., Lett.*, 2014, **783**, L4.
- 28 Y. Aikawa, E. Herbst, H. Roberts and P. Caselli, *Astrophys. J.*, 2005, **620**, 330.
- 29 K. Giers, S. Spezzano, F. Alves, P. Caselli, E. Redaelli, O. Sipilä, M. Ben Khalifa, L. Wiesenfeld, S. Brünken and L. Bizzocchi, *Astron. Astrophys.*, 2022, **664**, A119.



- 30 J. Cernicharo, C. A. Gottlieb, M. Guelin, T. C. Killian, P. Thaddeus and J. M. Vrtilik, *Astrophys. J., Lett.*, 1991, **368**, L43.
- 31 J. Cernicharo, M. Agúndez, C. Cabezas, N. Marcelino, B. Tercero, J. R. Pardo, R. Fuentetaja and P. de Vicente, *EPJ Web Conf.*, 2022, **265**, 00041.
- 32 B. A. McGuire, A. M. Burkhardt, R. A. Loomis, C. N. Shingledecker, K. L. K. Lee, S. B. Charnley, M. A. Cordiner, E. Herbst, S. Kalenskii, E. Momjian, E. R. Willis, C. Xue, A. J. Remijan and M. C. McCarthy, *Astrophys. J., Lett.*, 2020, **900**, L10.

